Supplementary material for

Marine flooding of a neotropical coastal lake during the 8.2-ka event

Jonathan Obrist-Farner, Mark Brenner, Jeffery R. Stone, Liseth Pérez, Marta Wojewódka, Thorsten Bauersachs, Andreas Eckert, Marek Locmelis, Jason H. Curtis, Susan R. H. Zimmerman, Alex Correa-Metrio, Lorenz Schwark, Edward Duarte, Antje Schwalb, Paula Gabriela Echeverría Galindo, and Etienne Niewerth

This PDF file includes:

Materials and Methods

Coring

Sediment cores were collected using two piston corers, one for unconsolidated mud-water interface (MWI) sediments (Fisher et al., 1992) and the other, a modified Livingstone corer, for deeper, consolidated sediments (Deevey, 1965). The cores were collected from a wooden platform mounted on two canoes. The MWI core was collected from the side of the platform to a sediment depth of 75 cm. The core was extruded in the field at 3.0-cm intervals and samples were placed in Whirl-Pak® bags. Next, a PVC casing pipe was lowered through a hole in the center of the platform and forced into the sediment to a depth of 1.0 m. Strong winds prevented us from controlling the depth to which we buried the casing pipe. We had intended to lower it only 0.5 m into the mud, and we hence have a gap of 25 cm between the base of the retrieved MWI core (75 cm) and the beginning of our next drive at 100 cm. Once the casing was set and cleaned, seven core sections were retrieved, to a depth of 760 cm. Sediment cores were kept inside the polycarbonate core barrels and transported to Missouri University of Science and Technology for further analysis. Cores at additional locations were collected from the wooden platform using the modified Livingstone piston corer. Rough weather conditions prevented us from collecting a MWI core at some sites. Cores 1-3 are incomplete.

Radiocarbon dating and age-depth modeling

Samples for radiocarbon dating were submitted to the Center for Accelerator Mass Spectrometry at Lawrence Livermore National Laboratory, California, USA and to Beta Analytic Inc., Florida, USA. All samples were first treated with a standard acid-base-acid treatment, graphitized, and their radiocarbon concentrations measured via Accelerator Mass Spectrometry. The age-depth model for core 5 was generated with an additional date (-68 cal yr BP; year of core collection with an intact mud-water interface) and extended to a depth of 760 cm (i.e., the maximum depth of core 5).

Core scans and photographs

Cores were scanned using a GEOTEK Multi-sensor core logger at two facilities. Cores were first scanned at the University of Florida, USA, at 1-cm resolution and later scanned at the National Lacustrine Core Facility (LacCore), University of Minnesota, USA, at 0.5-cm resolution (ST 6). Both instruments measured density and magnetic susceptibility. In addition, line-scan photographs were obtained. Sedimentological observations for core 5 were carried out on split core surfaces with the aid of the line-scan photographs (Schnurrenberger et al., 2003). Bed color (Munsell Color Chart, 2010), sedimentary textures and structures, as well as bedding planes were observed and recorded at 1-cm intervals. Bioturbation features were recorded following the bioturbation index classification (Taylor and Goldring, 1993).

X-ray fluorescence scanning

The split core from site 5 was analyzed at the Large Lakes Observatory, University of Minnesota, Duluth, USA, using an ITRAX XRF core scanner using a Cr source tube at 30 kV and 55 mA at 5-mm resolution with a 15-second dwell time. Raw data were reprocessed to optimize peak-fitting, using QSpec 8.6.0 software. In addition, X-radiographs were collected using a Cr source tube run at 60 kV and 30 mA, with variable exposure times, depending on the sediment density. All XRF data are reported in Table S6 and results were plotted using a 5-point moving average.

Sediment geochemistry

Samples for geochemical analysis were collected throughout core 5 at 5-cm intervals (i.e., ~ 50-year resolution) and every 3-cm for the MWI core (0-75 cm). All samples were oven dried at 60 °C for 24 h, ground to a fine powder, and placed in 20-ml scintillation vials. Total carbon (TC) was measured at University of Florida using a Carlo Erba NA1500 CNS elemental analyzer. Samples were loaded into tin capsules and placed in a 50-position automated Zero Blank sample carousel. After combustion in a quartz column at 1020 °C in an oxygen-rich atmosphere, the sample gas was transported in a He carrier stream and passed through a hot reduction column (650 °C) consisting of elemental copper, to remove oxygen. The effluent stream then passed through a chemical (magnesium perchlorate) trap to remove water, before entering a 0.7-m GC column at 120 °C, to separate N2 from CO2.

Carbonate carbon was measured coulometrically using a UIC (Coulometrics) 5017 CO2 coulometer coupled with an AutoMate automated carbonate preparation device (AutoMateFX.com). Fifteen mg of sample was weighed into septum-top tubes and placed into the AutoMate carousel. A double-needle assembly was used to purge the sample vial of atmospheric gas using CO2-free nitrogen carrier gas. Acid was then injected into the sample vial and evolved CO2 was carried through a silver nitrate scrubber to the coulometer where the C was measured. Total inorganic carbon (TIC) was determined assuming that all carbonate existed as CaCO3 and by multiplying the results of TIC by 8.33 (the stoichiometry of C in CaCO3). Total organic carbon (TOC) was calculated as the difference between TC and TIC.

For total sulfur (TS), 20 mg of bulk sediment was weighed into silver capsules along with ~10 mg of vanadium pentoxide. Capsules were crushed and placed in a 50-position autosampler carousel on a Carlo Erba NA1500 CNS Elemental Analyzer. Samples were flash combusted at 1020 °C in an oxygen-rich atmosphere in the top portion of a quartz column containing tungstic anhydride. The bottom portion of the same column (also at 1020 °C) contained pure copper wires to remove oxygen. The sample gas was transported in a He carrier stream that then passed

through a chemical (magnesium perchlorate) trap to remove water. The stream then passed through a 0.8-m gas chromatographic column at 75°C that separates SO2 from N2 and CO2. Finally, the gases passed through a thermal conductivity detector that measures the size of the pulses of SO2. All geochemical results are given in Table S6.

Diatom analysis

Diatom samples were taken at 20-cm intervals (~200-year resolution), dried at low temperature in an oven, weighed into glass scintillation vials, and digested with 10 mL of 30% hydrogen peroxide at room temperature for 2-3 weeks. After digestions were complete, samples were rinsed four times with DIW, spiked with a known concentration of microspheres, dried onto coverslips, and mounted to microscope slides using Naphrax (Battarbee, 2003). When possible, at least 300 diatoms were identified and enumerated in each sample, using a 100x objective (1000x total magnification) with differential interference contrast, on a compound light microscope. After major stratigraphic changes in diatom assemblages were identified, sample resolution was increased to 10-cm intervals across the marine incursion and across the interval where lake biota recovered.

Biomarker analysis

Seventeen samples were collected from core 5 for biomarker analyses. All samples were lyophilized for 24 h and ground to a fine powder using a solvent-cleaned agate pestle and mortar. Aliquots of the homogenized sediments (0.4 to 2.5 g) were Bligh and Dyer extracted as described previously (Papadomanolaki et al., 2018).

An aliquot (~0.5 to 2 mg) of each lipid extract was separated by Al_2O_3 column chromatography into apolar and polar lipid fractions using n-hexane:dichloromethane (9:1; v:v) and dichloromethane:methanol (1:1; v:v), respectively. The polar fractions, containing glycerol dialkyl glycerol tetraethers (GDGTs), was dissolved in a solvent mixture of n-hexane:2-propanol (99:1; v:v) to a concentration of 2 mg ml^{-1} and filtered through a 0.45 µm polytetrafluoroethylene (PTFE) filter (Macherey-Nagel, Germany) prior to analysis by high-performance liquid chromatography coupled to mass spectrometry (HPLC-MS) at Christian-Albrechts-University. Briefly, GDGTs were eluted at 30 °C using a Waters Alliance 2695 HPLC system fitted with two BEH HILIC silica columns (2.1 × 150 mm, 1.7 µm; Waters) and a guard column of the same material. The gradient program of Hopmans et al. (2016) was applied. Detection of GDGTs was achieved using a Micromass ZQ single quadrupole mass spectrometer equipped with an atmospheric pressure chemical ionization interface operated in positive ion mode. Source conditions were as described in Weidenbach et al. (2017). GDGTs were recorded by selected ion monitoring (SIM) of their [M+H]+ ions (dwell time = 200 ms) according to Hopmans et al. (2000) and quantified by integration of peak areas using the QuanLynx integration software of MassLynx (Version 4.1 SCN856). The GDGT-0/crenarchaeol ratio was calculated and interpreted following Blaga et al. (2009).

Supplementary Figures

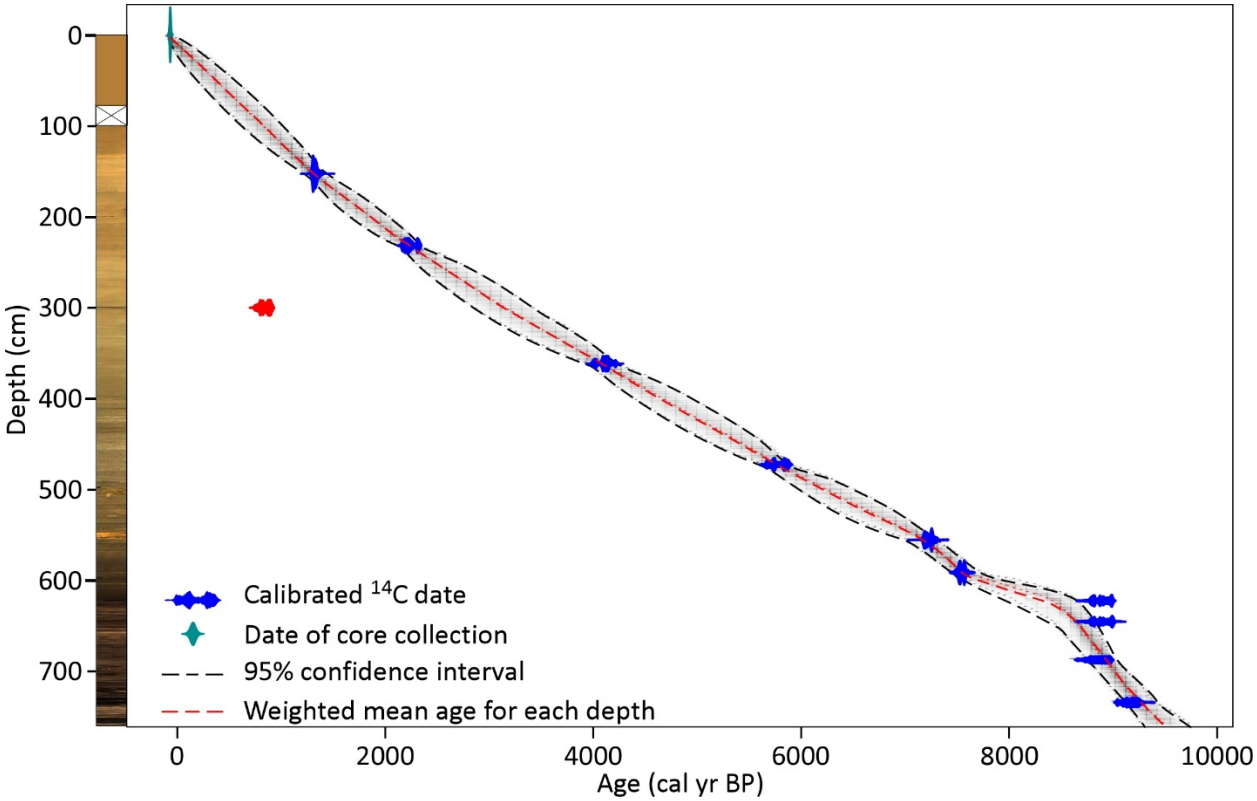

Supplementary Figure 1. Age-depth model for core 5 from Lake Izabal, based on 10 calibrated AMS radiocarbon dates (dark blue) and the date of coring (green; -68 cal yr BP). Red line shows the best-fit model based on weighted mean ages, and stippled gray lines show 95% confidence intervals. All dates were calibrated using IntCal20 (Reimer et al., 2020). The age-depth model was generated using Bacon (Blaauw & Christen, 2011) and redrawn. The sample marked in red was excluded because the wood fragment was near the top of a core section and likely out of place.

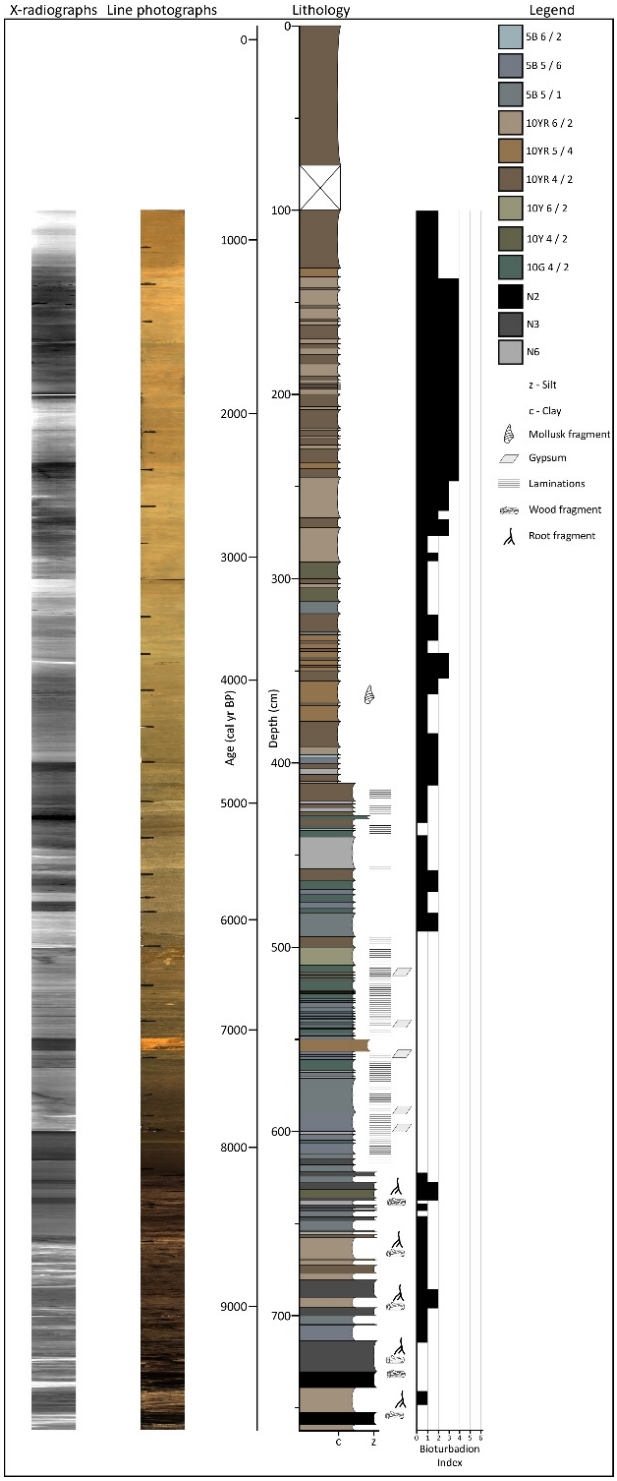

Supplementary Figure 2. X-radiographs, line scan photographs, and lithology, textural, and structural description of core 5 from Lake Izabal. Notice the persistence of laminae from ~8,200 to ~6,000 cal yr BP and their sporadic presence until ~4,800 cal yr BP. Few bioturbated intervals are present at ~6000 cal yr BP, but become a significant part of the record after ~4,800 cal yr BP.

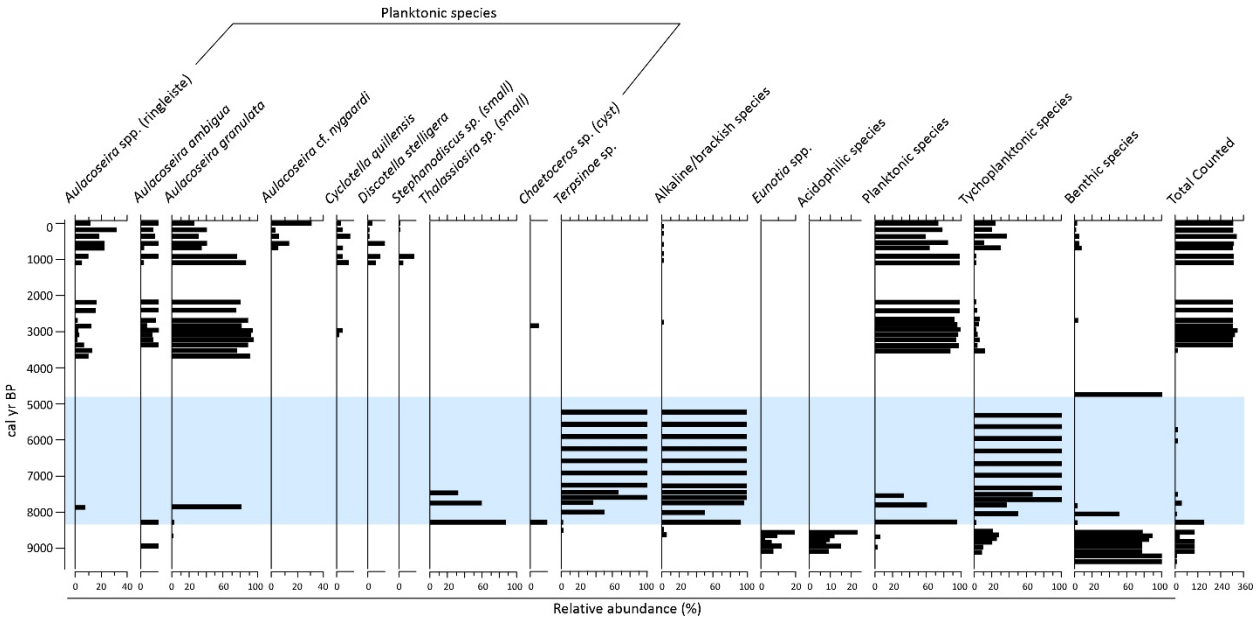

Supplementary Figure 3. Relative abundances (%) of selected diatom taxa and total diatoms counted in samples from core 5 in Lake Izabal. All species shown in Supplementary Table 4. Diatoms were extremely scarce in sediments deposited after the marine incursion at ~8,300 cal yr BP, accounting for the low total counts. Some taxa disappeared completely during the subsequent ~4,800 years. After ~3,500 cal yr BP, diatoms were generally more abundant, enabling total counts in samples of ~250-300 frustules. The blue zone highlights the interval of marine incursion and hypersaline, reducing conditions in Lake Izabal.

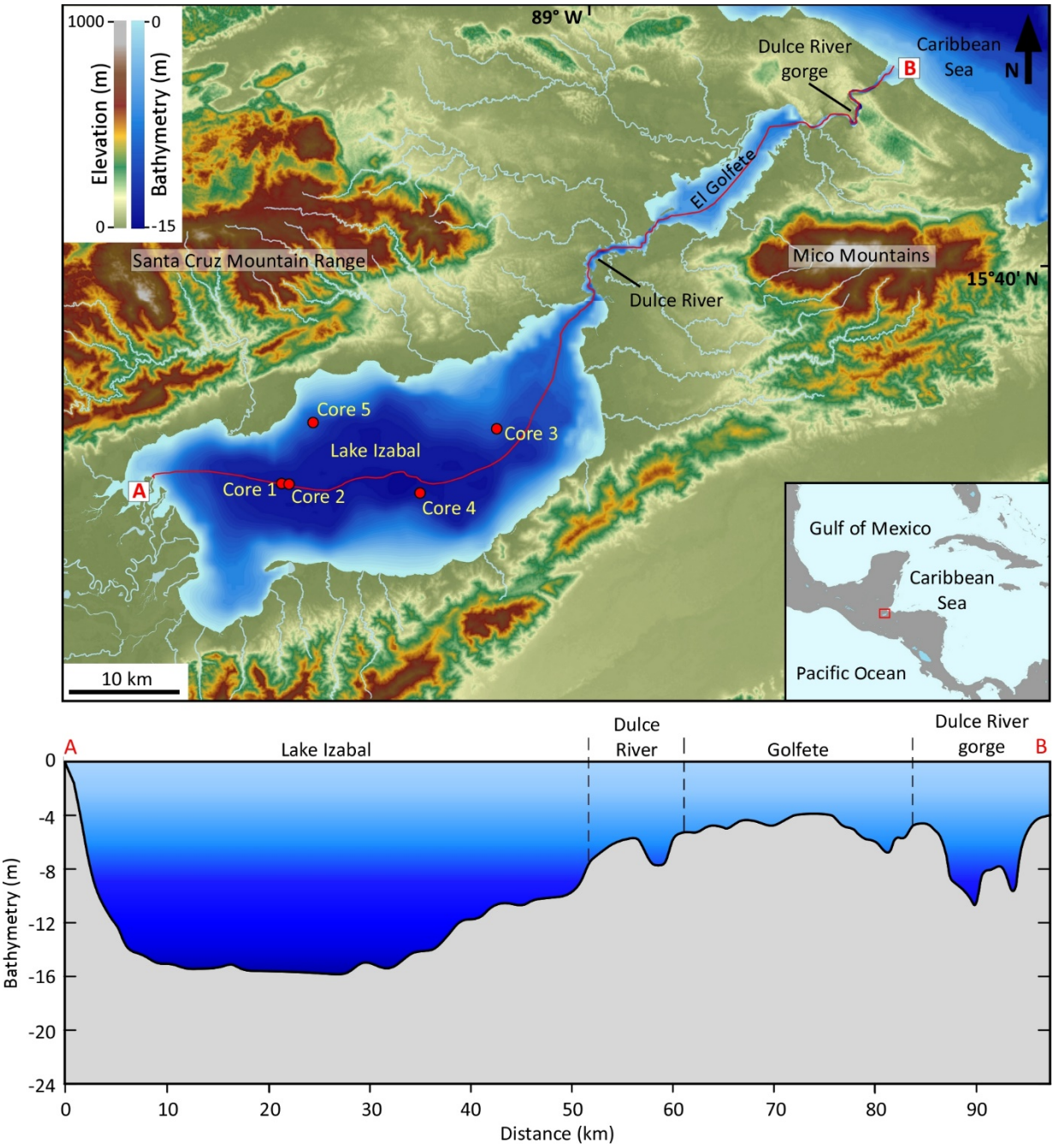

Supplementary Figure 4. Top panel shows the bathymetric map of Lake Izabal and topography of the area. Red circles indicate sites of sediment core collection. The red line shows the location of the cross section shown in the bottom panel. The inset map shows Central America and surrounding regions, with the location of Lake Izabal in eastern Guatemala indicated by the red box. Bottom panel shows the bathymetric cross-section across the Lake Izabal system with a vertical exaggeration of 1300. The cross section has been smoothed to show the general features of the area. Current bathymetric information indicates that the highest point of the system is Lake El Golfete.

References

Battarbee, R. W., 2003, Diatom analysis, *in* Berglund, B. E., and Ralska-Jasiewiczowa, M., eds., Handbook of Holocene palaeoecology and palaeohydrology: New Jersey, Blackburn Press, p. 527-570.

Blaauw, M., and Christen, J. A., 2011, Flexible paleoclimate age-depth models using an autoregressive gamma process: Bayesian Analysis, v. 6, p. 457-474.

Blaga, C. I., Reichart, G.-J., Heiri, O., and Sinninghe Damsté, J. S., 2009, Tetraether membrane lipid distributions in water-column particulate matter and sediments: a study of 47 European lakes along a north–south transect: Journal of Paleolimnology, v. 41, p. 523-540.

Deevey, E. S., 1965, Sampling lake sediments by use of the Livingstone sampler, *in* Kummel, B., and Raup, D., eds., Handbook of paleontological techniques: San Francisco, Freeman, p. 521-529.

Fisher, M. M., Brenner, M., and Reddy, K. R., 1992, A simple, inexpensive piston corer for collecting undisturbed sediment/water interface profiles: Journal of Paleolimnology, v. 7, p. 157-161.

Hopmans, E. C., Schouten, S., Pancost, R. D., van der Meer, M. T. J., and Sinninghe Damsté, J. S., 2000, Analysis of intact tetraether lipids in archaeal cell material and sediments by high performance liquid chromatography/atmospheric pressure chemical ionization mass spectrometry: Rapid Communications in Mass Spectrometry, v. 14, p. 585-589.

Hopmans, E. C., Schouten, S., and Sinninghe Damsté, J. S., 2016, The effect of improved chromatography on GDGT-based palaeoproxies: Organic Geochemistry, v. 93, p. 1-6.

Munsell Color Chart, 2010, Munsell soil color charts: with genuine Munsell color chips. Grand Rapids, MI.

Papadomanolaki, N. M., Dijkstra, N., van Helmond, N. A. G. M., Hagens, M., Bauersachs, T., Kotthoff, U., Sangiorgi, F., and Slomp, C. P., 2018, Controls on the onset and termination of past hypoxia in the Baltic Sea: Palaeogeography, Palaeoclimatology, Palaeoecology, v. 490, p. 347-354.

Reimer, P. J., Austin, W. E. N., Bard, E., Bayliss, A., Blackwell, P. G., Bronk Ramsey, C., Butzin, M., Cheng, H., Edwards, R. L., Friedrich, M., Grootes, P. M., Guilderson, T. P., Hajdas, I., Heaton, T. J., Hogg, A. G., Hughen, K. A., Kromer, B., Manning, S. W., Muscheler, R., Palmer, J. G., Pearson, C., van der Plicht, J., Reimer, R. W., Richards, D. A., Scott, E. M., Southon, J. R., Turney, C. S. M., Wacker, L., Adolphi, F., Büntgen, U., Capano, M., Fahrni, S. M., Fogtmann-Schulz, A., Friedrich, R., Köhler, P., Kudsk, S., Miyake, F., Olsen, J., Reinig, F., Sakamoto, M., Sookdeo, A., & Talamo, S., 2020, The IntCal20 Northern Hemisphere radiocarbon age calibration curve (0–55 cal kBP): Radiocarbon, v. 62, p. 725-757.

Schnurrenberger, D., Russell, J., and Kelts, K., 2003, Classification of lacustrine sediments based on sedimentary components: Journal of Paleolimnology, v. 29, p. 141-154.

Taylor, A. M., and Goldring, R., 1993, Description and analysis of bioturbation and ichnofabric: Journal of the Geological Society, v. 150, p. 141-148.

Weidenbach, K., Nickel, L., Neve, H., Alkhnbashi, O. S., Künzel, S., Kupczok, A., Bauersachs, T., Cassidy, L., Tholey, A., Backofen, R., and Schmitz, R. A., 2017, MetSV, a novel archaeal lytic virus targeting Methanosarcina strains: Journal of Virology, JVI.00955-00917.

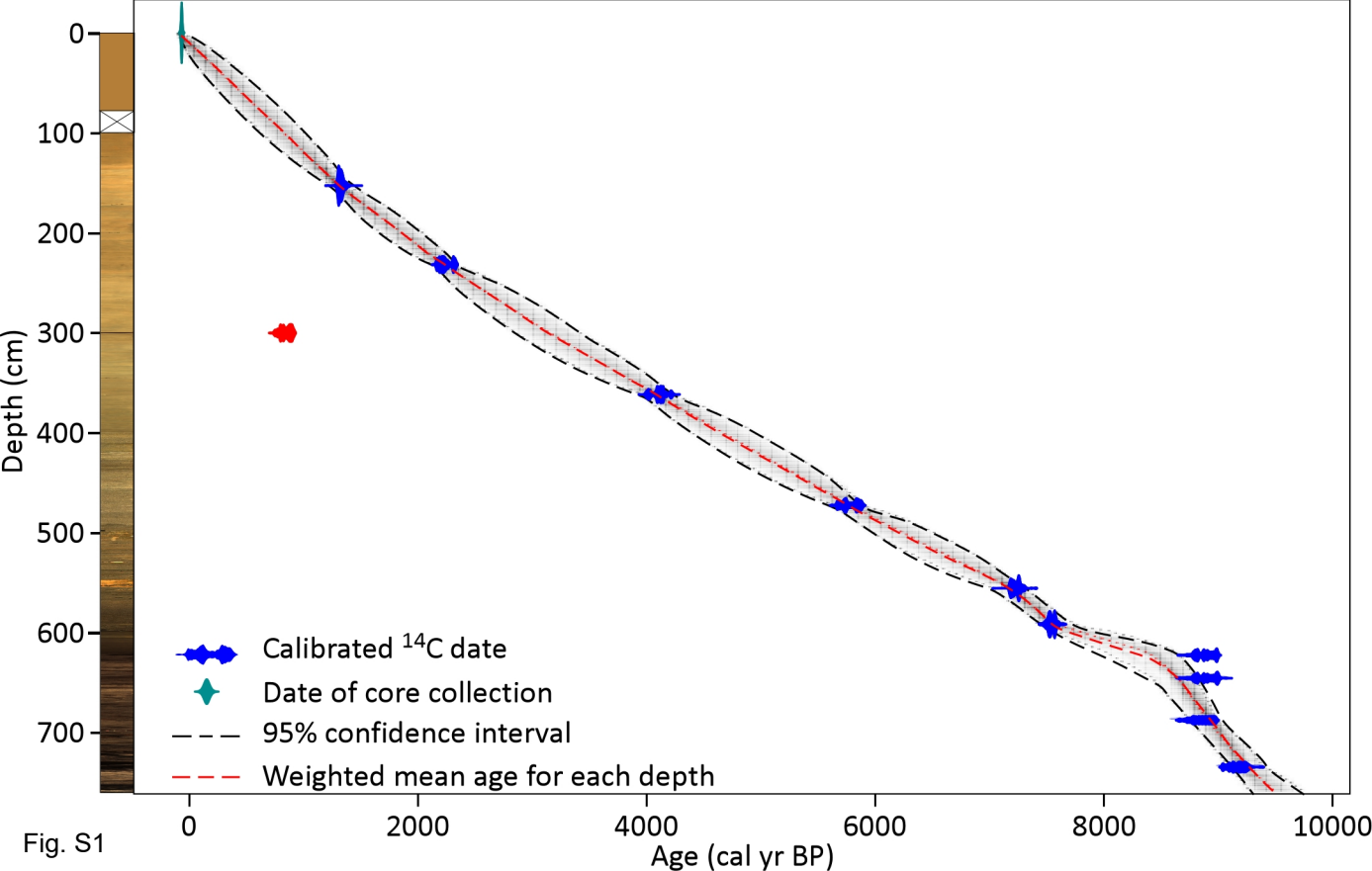
Depth (cm)
0
100
200
300
400
500
600
700
0
2000
4000
6000
8000
10000
Age (cal yr BP)
Calibrated ^{14}C date
Date of core collection
95% confidence interval
Weighted mean age for each depth

Fig. S1

X-radiographs Line photographs Lithology Legend

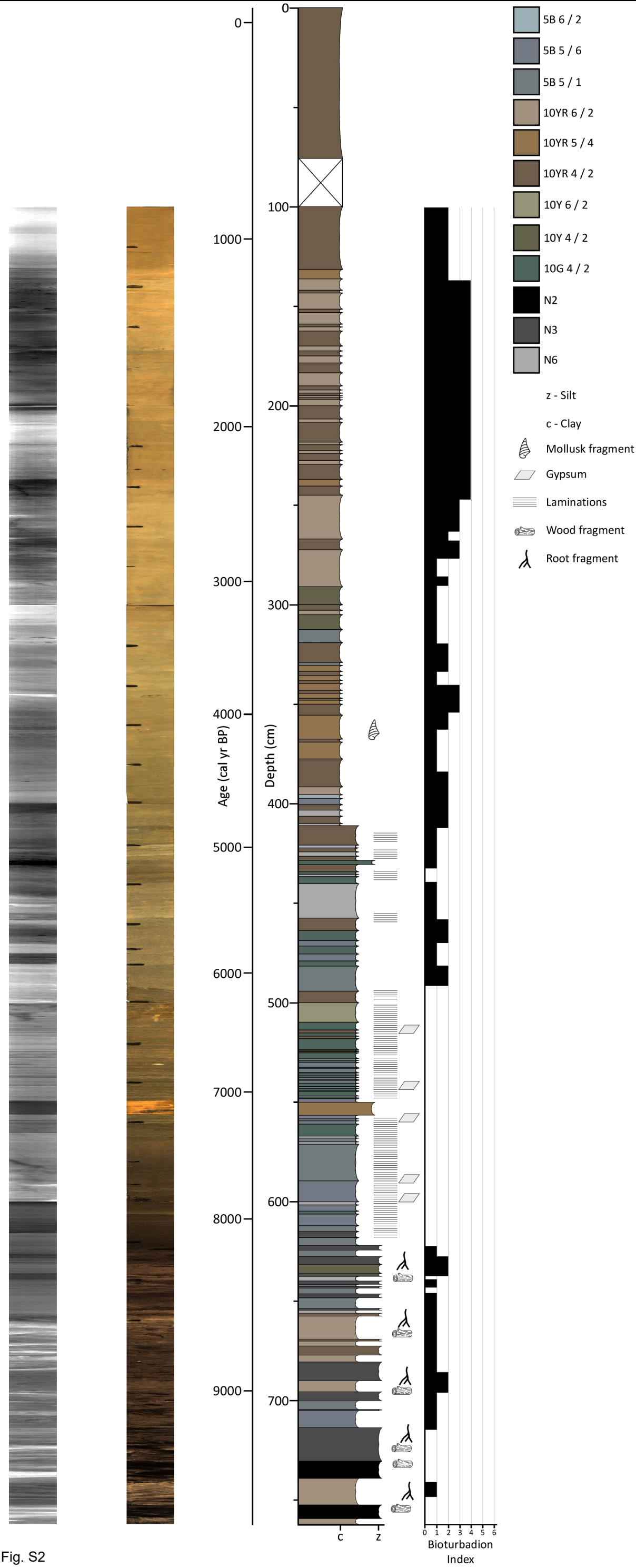

Fig. S2

Fig. S3

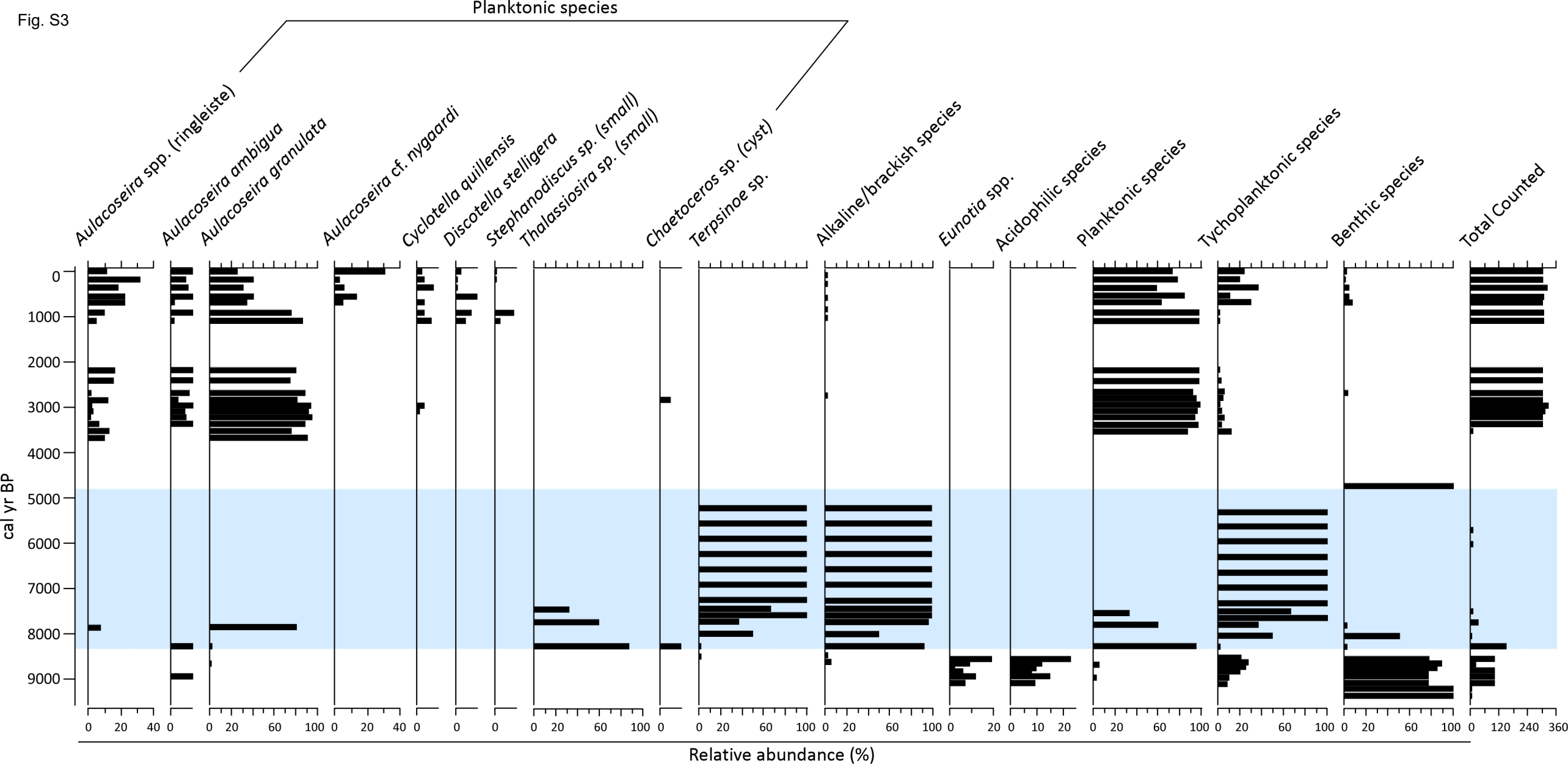
Planktonic species
Aulacoseira spp. (ringleiste)
Aulacoseira ambigua
Aulacoseira granulata
Aulacoseira cf. nygaardi
Cyclotella quillensis
Discotella stelligera
Stephanodiscus sp. (small)
Thalassiosira sp. (small)
Chaetoceros sp. (cyst)
Terpsinoe sp.
Alkaline/brackish species
Eunotia spp.
Acidophilic species
Planktonic species
Tychoplanktonic species
Benthic species
Total Counted
cal yr BP
0
1000
2000
3000
4000
5000
6000
7000
8000
9000
0 20 40
0 20 60 100
0 20 40
0
0
0
0 20 60 100
0
0 20 60 100
0 20 60 100
0 20
0 10 20
0 20 60 100
0 20 60 100
0 20 60 100
0 120 240 360
Relative abundance (%)

Fig. S4

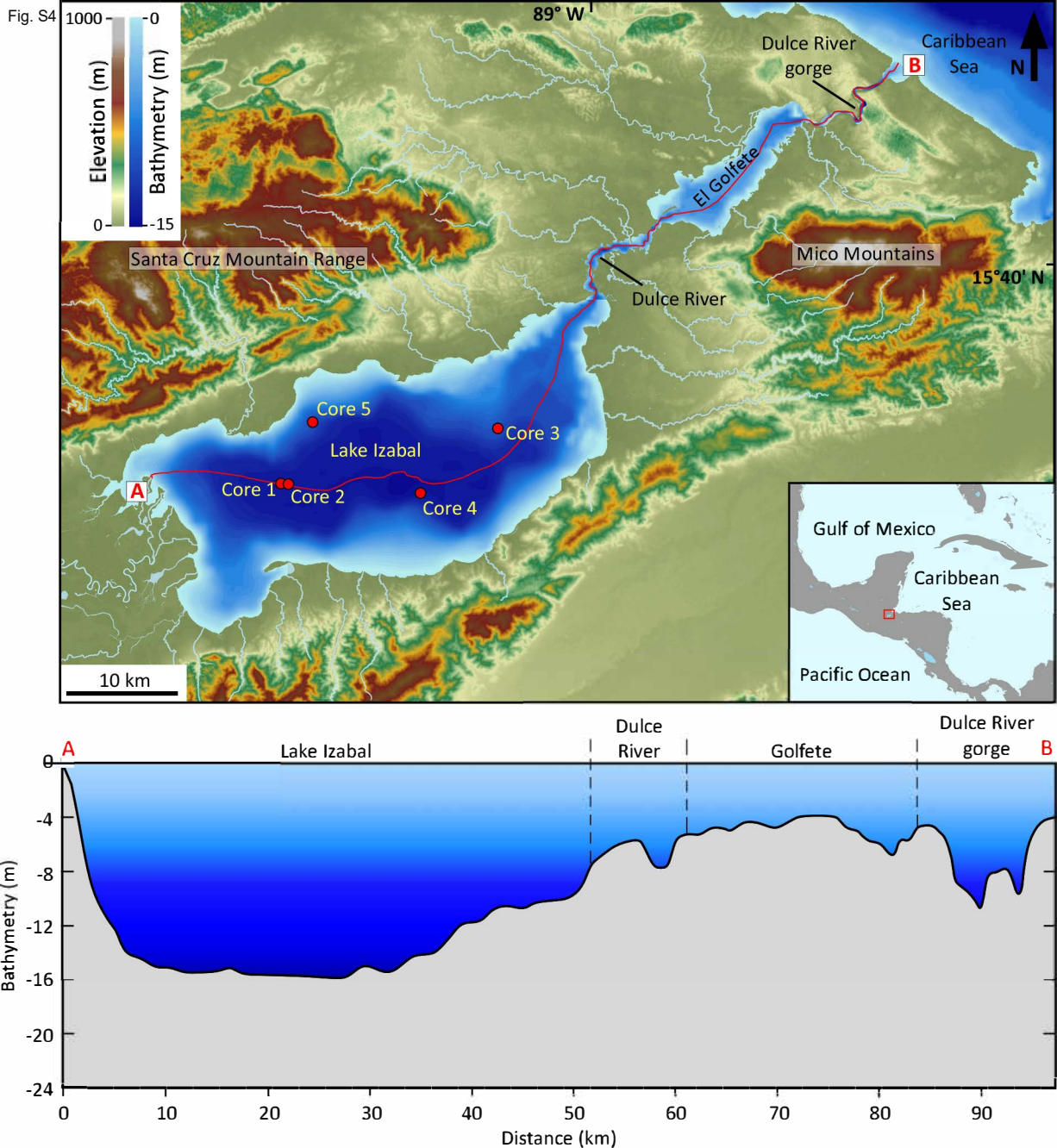
1000
0
Elevation (m)
0
-15
Bathymetry (m)
89° W
Dulce River gorge
B
Caribbean Sea
N
El Golfete
Santa Cruz Mountain Range
Mico Mountains
15°40' N
Dulce River
Core 5
Core 3
Lake Izabal
A
Core 1
Core 2
Core 4
Gulf of Mexico
Caribbean Sea
Pacific Ocean
10 km
A
Lake Izabal
Dulce River
Golfete
Dulce River gorge
B
0
-4
-8
-12
-16
-20
-24
Bathymetry (m)
0
10
20
30
40
50
60
70
80
90
Distance (km)